Available online at www.sciencedirect.com

SciVerse ScienceDirect

Ceramics International 39 (2013) 3409–3412

CERAMICS INTERNATIONAL

www.elsevier.com/locate/ceramint

Short communication

Synthesis of zirconium carbide powders using chitosan as carbon source

Chunlei Yan, Rongjun Liu*, Yingbin Cao, Changrui Zhang, Deke Zhang

Science and Technology on Advanced Ceramic Fibers and Composites Laboratory, National University of Defense Technology, Changsha 410073, China

Received 4 August 2012; received in revised form 8 September 2012; accepted 8 September 2012
Available online 18 September 2012

Abstract

Chitosan–zirconium complex, obtained by chelation of chitosan to zirconium, formed a novel precursor for zirconium carbide (ZrC). ZrC was synthesized via carbothermal reduction reaction using zirconium oxychloride ($ZrOCl_2 \cdot 8H_2O$), and chitosan as sources of zirconium and carbon. The initiation of carbothermal reduction process was at about 1400 °C, and the reaction was substantially completed at a relatively lower temperature (~1550 °C), compared with that using $ZrOCl_2 \cdot 8H_2O$ and phenolic resin as a carbon source. The conversions from as-synthesized preceramic precursors to ceramics were studied by means of FTIR, DSC-TG, SEM, EDS and XRD.

Keywords: Zirconium carbide; Inorganic–organic hybrid precursor; FTIR; X-ray techniques

1. Introduction

Zirconium carbide (ZrC) is one of the refractory transition metal carbides from groups IV to V of the periodic table. It has high melting point (~3420 °C), high hardness (~25.5 GPa), and weak damage sensitivity under irradiation, which make it suitable for many applications such as field emitters, coating of nuclear particle fuels and cutting tools [1,2]. Also, by addition of SiC or ZrB_2 to increase the oxidation resistance, ZrC-based ceramics are expected to be good potential materials for ultra-high temperature applications [3].

ZrC powders can be conventionally prepared by the carbothermal reduction of ZrO_2 or the direct reaction of Zr with C at elevated temperatures. However, a high temperature and a long production period are required for above mentioned methods. The sol–gel method is an effective way for low-temperature synthesis of ultra-fine powders for the intimate contact of the reactants, but there are still several drawbacks such as high cost, toxicity, and poor stability of the sol [4,5].

Chitin is the second most abundant polysaccharide found on earth next to cellulose. The most important derivative of chitin is chitosan. Unlike chitin, chitosan is soluble in dilute organic acids such as acetic acid, formic acid, lactic acid, etc. Both chitin and chitosan are becoming increasingly important natural polymers because of the interest in natural resources and environment-friendly processes [6–8]. Besides, chitosan has the highest chelating ability in comparison with other natural polymers. The high content of nitrogen atoms in the molecular allows uptake of several metal ions through various mechanisms such as chelation, electrostatic attraction or ion-exchange [9]. Chitosan and its degradation behavior in various conditions have been extensively investigated. At high temperatures, chitosan usually produces char and some volatile compounds under an inert atmosphere [10]. Herein, we expect that the chitosan–metal complexes, obtained from chitosan and transition metal salts, will be promising precursors for transition metal carbides. In this paper, we report the convenient one-pot synthesis of ZrC using $ZrOCl_2 \cdot 8H_2O$ and chitosan as sources of zirconium and carbon, respectively. For comparison, synthesis of ZrC using $ZrOCl_2 \cdot 8H_2O$ and phenolic resin will be also carried out.

2. Experimental

Chitosan (degree of deacetylation ≥ 90%), whose char yield was about 30 wt% according to the results of TG curve, was purchased from Shang Hai Bio Science & Technology

*Corresponding author. Tel.: +86 731 84573169; fax: +86 731 84576433.
E-mail address: rongjunliu@nudt.edu.cn (R. Liu).

0272-8842/$ - see front matter © 2012 Elsevier Ltd and Techna Group S.r.l. All rights reserved.
http://dx.doi.org/10.1016/j.ceramint.2012.09.032

Co., Ltd. The char yield of phenolic resin was about 60 wt%. Zirconium oxychloride octahydrate and acetic acid were of analytical grade.

First, $ZrOCl_2 \cdot 8H_2O$ was dissolved in distilled water to form a solution, and then chitosan was added to the solution with stirring using various C/Zr molar ratios. In order to dissolve chitosan in water, a certain amount of acetic acid was added, next, the mixture was stirred at 80 °C until a clear solution formed. As a comparison, synthesis of ZrC was also carried out using $ZrOCl_2 \cdot 8H_2O$ and phenolic resin (50 wt% in ethanol). All samples for pyrolysis should be dried at 180 °C for the purpose of volatilization of the solvent. Finally, pyrolysis was carried out in a graphite furnace which was heated in vacuum to 250 °C and then in flowing argon (purity 99.999%) to the required temperatures in the range of 1200–1550 °C, and held for 2 h.

Fourier transform infrared spectra (FTIR, Avatar 360, Nicolet) of the chitosan–zirconium complex and starting reagents were recorded between 4000 and 400 cm^{-1} so as to monitor structural changes during heating. The phase compositions were determined using X-ray diffraction (XRD, TTR-3, Rigaku) with Cu K_α radiation. The pyrolysis of chitosan and zirconium–chitosan complex was studied by differential scanning calorimetry and thermal gravimetric analysis (DSC-TG, Netzsch STA 449C) in an argon atmosphere at a heating rate of 10 °C/min. The particle size and morphology of the final products were characterized by scanning electron microscopy (S4800 Hitachi).

3. Results and discussion

Spectroscopy in the infrared region was used to monitor structural changes and the principal interactions between chitosan and the metal ion during heat treatment (Fig. 1). In the FTIR curve of as-received $ZrOCl_2 \cdot 8H_2O$, the band at 1623 cm^{-1} may be assigned to the "scissor" bending mode of coordinated water. For chitosan, the respective assignments of the absorption peaks are 3440 (ν(O–H)+ν(N–H)), 2885 (ν(C–H)), 1649 (amide I band, ν(C=O)), 1596 (amide II band, δ(N–H)), 1384(δ(C–H)), 1079 (ν(C–O)) cm^{-1} [11]. Fig. 1(c) shows the FTIR spectrum of chitosan–zirconium complex dried at 180 °C. The spectrum exhibits many alterations from that of chitosan. The wide peak at 3440 cm^{-1} attributed to the stretching vibration of $–NH_2$ and –OH groups shifts to lower wavenumber, indicating $–NH_2$ and –OH groups take part in complexation. Absorption bands at 1649 cm^{-1} assigned to acetamide group and 1596 cm^{-1} assigned to "free" amine group disappear in the complexes. Instead, a new angular absorption band at 1560 cm^{-1} appears, which is considered as a characteristic peak of the association of chitosan and metal. The two strong absorption bands at 1456, 1416 cm^{-1} are attributed to the C–H bending vibration and the –C–N– stretching vibration of the residual amide, respectively. The band (1079 cm^{-1}) assigned to the second –OH group shows a significant shift to lower wavenumber (1022 cm^{-1}), combined with the results discussed by Patale and Patravale [12],

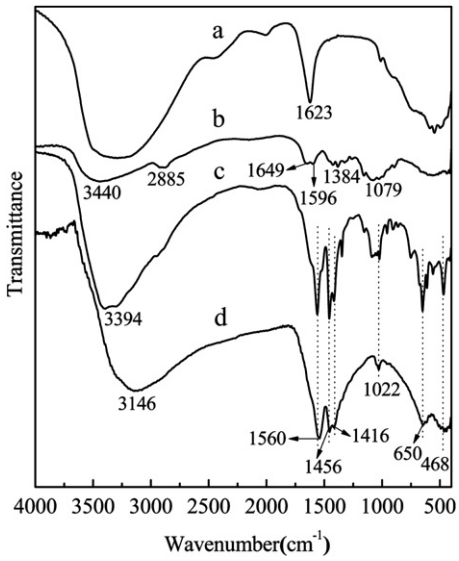

Fig. 1. FTIR spectra of starting reagents and chitosan–zirconium complex: (a) as-received $ZrOCl_2 \cdot 8H_2O$; (b) chitosan; (c) chitosan–zirconium complex dried at 180 °C in air and (d) 250 °C in vacuum.

suggesting that the second –OH group gets involved in complexation. Two new peaks located at 650, 468 cm^{-1}, which are attributed to ring distortion + ν(Zr–O) of the cyclic structure after Zr (IV) ion chelation and ν(Zr–O)+ν(Zr–N), respectively [13], appear in the FTIR curve of the chitosan–zirconium complex. Two hypothetical models for the structures of chitosan–metal complexes have been experimentally proved [9] and agree well with the above mentioned results. When the temperature is elevated to 250 °C in vacuum, the spectrum exhibits many resemblances compared with that of the complex dried at 180 °C. However, all the peaks at 3146, 1560, 1456, 1416, 1022, 650, 468 cm^{-1} get broader and weaker. Moreover, the peak at 2885 (ν(C–H)) cm^{-1} disappears, suggesting that the chitosan in complex could be dehydrated, and then in situ carbonized during heating, although the chelated structures still maintain. This is very important for achievement of the homogeneous and intimate mixing of components for the carbothermal reaction.

The thermal degradation behavior of chitosan has been studied by simultaneous TG and DSC (Fig. 2(a)). TG analysis shows that a considerable weight loss occurs at about 73 °C due to the evaporation of water absorbed in chitosan, which results in an apparent endothermic peak in the DSC curve. The weight loss between 200 and 400 °C is thought to be attributed to the cross-linking and degradation of chitosan, as a result, an apparent exothermic peak appears at 305 °C. After 600 °C, the weight loss tends to stabilize, and the maximal weight loss is about 69.2% at 980 °C. Fig. 2(b) shows the TG-DSC curves of chitosan–zirconium complex powders. The two endothermic peaks located at 75, 181 °C in the DSC curve are attributed to the evaporation of water absorbed in chitosan and the bonded water in $ZrOCl_2 \cdot 8H_2O$. TG analysis shows that a significant weight loss occurs at about 242 °C, which is thought to be attributed to the cross-linking of chitosan and the further

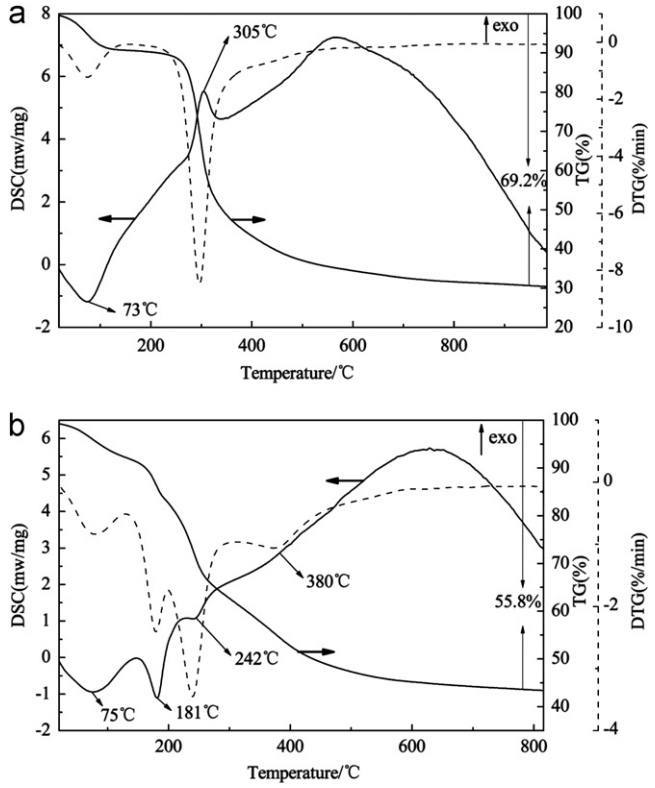

Fig. 2. DSC-TG curves of as-received chitosan powders (a) and (b) chitosan–zirconium complex dried at 180 °C.

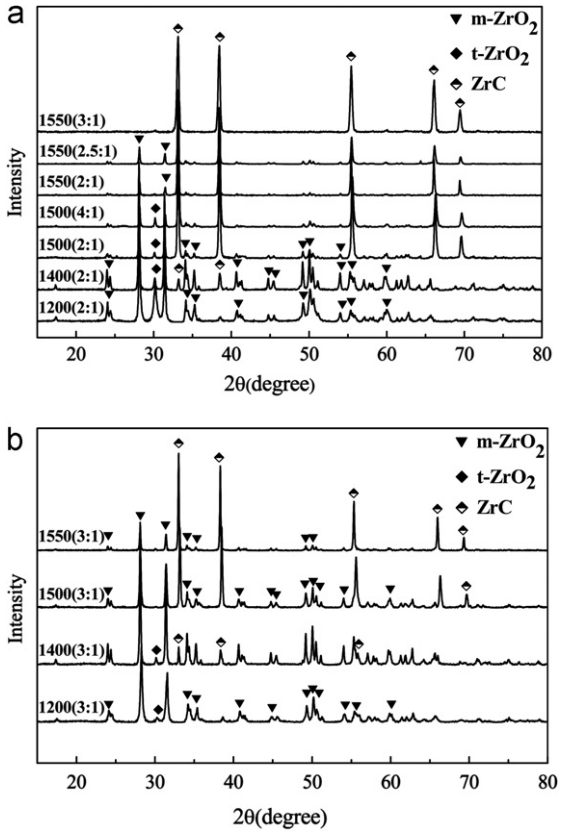

Fig. 3. XRD patterns of the hybrid precursors for ZrC: (a) chitosan–zirconium complex; (b) $ZrOCl_2 \cdot 8H_2O$ + phenolic resin using various C/Zr molar ratios (in brackets) at different heat treatment temperatures (°C).

evaporation of the bonded water in $ZrOCl_2 \cdot 8H_2O$. The main weight loss of complex occurs below 500 °C, and the maximal weight loss is about 55.8 wt% at about 800 °C. Finally, zirconia and char form and can be regarded as reagents for the subsequent carbothermal reduction.

XRD patterns of the hybrid precursors for ZrC using chitosan and phenolic resin as carbon source at different heat treatment temperatures are shown in Fig. 3(a) and (b), respectively. XRD patterns of both pyrolyzed precursors show that at temperatures below 1400 °C, only ZrO_2 exists without ZrC formation, and the carbon in the sample remains amorphous. The initial formation of ZrC is observed in both pyrolyzed precursors at 1400 °C that is much lower than the conventional solid state synthesis method, indicating that carbothermal reduction process is initiated as shown in Fig. 4. The intensity of *m*-ZrO_2 and *t*-ZrO_2 gradually decreases with the rise of temperature, and ZrC becomes the predominant phase at the temperatures higher than 1500 °C. For the precursor using chitosan as carbon source, *m*-ZrO_2 and *t*-ZrO_2 exist simultaneously at heat treatment temperatures below 1500 °C. Although C/Zr molar ratio increases to 4, the precursor cannot completely transform into ZrC after heat treatment at 1500 °C. XRD patterns at 1550 °C show that only m-ZrO_2 exists with C/Zr molar ratio below 3, indicating that some t-ZrO_2 has transformed into m-ZrO_2. Furthermore, the intensity of ZrC increases with the rise of C/Zr molar ratio, and ZrC is the only crystalline phase with C/Zr molar ratio of 3. However, the pyrolyzed precursor using phenolic resin still has a considerable amount of ZrO_2 using the same C/Zr molar ratio. The reason may lie in the chitosan for its high chelating ability. The FTIR spectra of chitosan–zirconium complex have indicated that the chitosan is dehydrated and in situ carbonized partially when the temperature is elevated to 250 °C in vacuum. We can deduce that the maintenance of chelation will hold until the chitosan is completely carbonized. Therefore, a more homogeneous and intimate mixing of components (atomic-scale or at least molecular-scale mixing) is achieved with a short diffusing path for carbothermal reduction. On the other hand, for the precursor that using $ZrOCl_2 \cdot 8H_2O$ and phenolic resin, because phenolic resin can hardly react with $ZrOCl_2 \cdot 8H_2O$ or coordinate to Zr atom, carbon pyrolyzed by phenolic resin may form aggregates after the evaporation of solvent, then give a long diffusing path to react with ZrO_2, so higher temperatures are required for carbothermal process.

Microstructures of the ceramic prepared from chitosan–zirconium complex are shown in Fig. 5(a). ZrC powders exhibit irregular polyhedron morphology with rather smooth crystal plane, and there are evident boundaries among grains. Particle sizes appear in the range of 2–5 μm. As shown in Fig. 5(b), only Zr and C and a trace of O (~3.0 at%) are detected by EDS analysis, indicating that the precursor has almost entirely been transformed into ZrC. This result agrees well with that of XRD analysis.

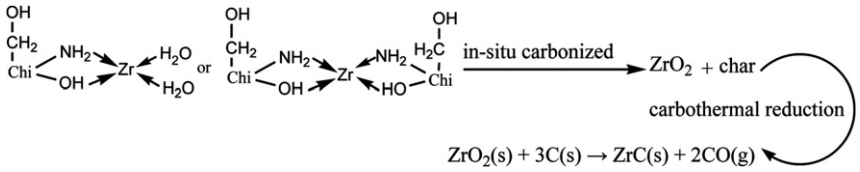

Fig. 4. The possible molecular structures of chitosan–metal complex and the carbothermal reduction process (Chi = Chitosan).

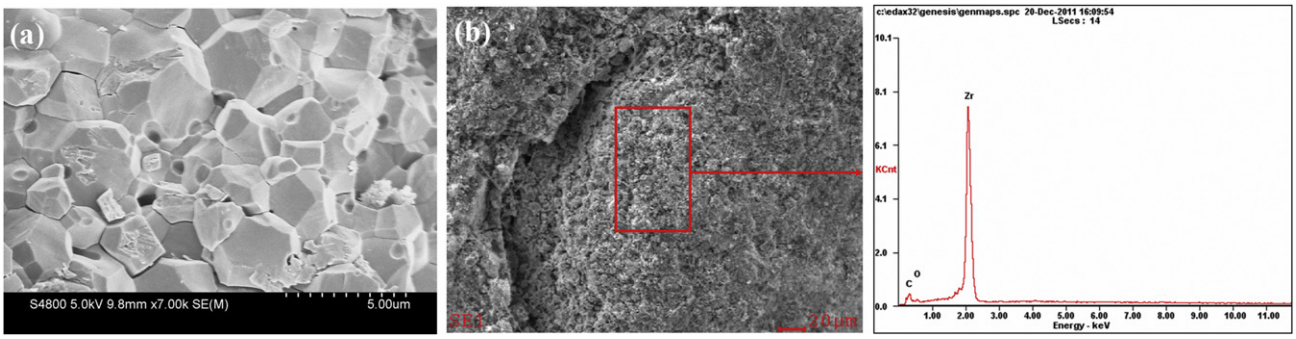

Fig. 5. (a) SEM micrograph of ZrC powders synthesized from chitosan–zirconium complex at 1550 °C and (b) EDS spectrum of as-received ZrC in (a).

4. Conclusions

Zirconium carbide powders have been successfully synthesized using chitosan–zirconium complex as a novel precursor. The chitosan in the chitosan–zirconium complex, whose char yield was about 30 wt%, was in situ carbonized when the complex was heat treated. Based on the results, the carbothermal reaction was substantially completed at a relatively lower temperature (~1550 °C) with C/Zr molar ratio of 3 for the homogeneous and intimate mixing of components (namely ZrO_2 and pyrolyzed C), compared with that using $ZrOCl_2 \cdot 8H_2O$ and phenolic resin as a carbon source. The synthesized powders had a small average particle size (~3 μm), and an oxygen content of ~3.0 at%. The low-temperature and environment-friendly synthesis of ZrC powders and the unlimited supply of chitosan will make the precursor to be widely used in ZrC preparation for sintering of ZrC-based ceramics.

Acknowledgments

We gratefully acknowledge the financial support of National Natural Science Foundation of China (51102282).

References

[1] D. Sciti, S. Guicciardi, M. Nygren, Spark plasma sintering and mechanical behavior of ZrC-based composites, Scripta Materialia 59 (2008) 638–641.
[2] K. Minato, T. Ogawa, K. Sawa, A. Ishikawa, T. Tomita, S. Iida, H. Sekino, Irradiation experiment on ZrC-coated fuel particles for high temperature gas-cooled reactors, Nuclear Technology 130 (2000) 272–281.
[3] Q.G. Li, S.M. Dong, Z. Wang, P. He, H.J. Zhou, J.S. Yang, B. Wu, J.B. Hu, Fabrication and properties of 3-D C_f/SiC–ZrC composites, using ZrC precursor and polycarbosilane, Journal of the American Ceramic Society 95 (4) (2012) 1216–1219.
[4] M. Dollé, D. Gosset, C. Bogicevic, F. Karolak, D. Simeone, G. Baldinozzi, Synthesis of nanosized zirconium carbide by a sol-gel route, Journal of the European Ceramic Society 27 (2007) 2061–2067.
[5] Y.J. Yan, Z.R. Huang, X.J. Liu, D.L. Jiang, Carbothermal synthesis of ultra-fine zirconium carbide powders using inorganic precursors via sol-gel method, Journal of the Sol–Gel Science and Technology 44 (2007) 81–85.
[6] R. Jayakumara, D. Menona, K. Manzoora, S.V. Naira, H. Tamura, Biomedical applications of chitin and chitosan based nanomaterials—a short review, Carbohydrate Polymer 82 (2010) 227–232.
[7] J. Kumirska, M. Czerwicka, Z. Kaczyński, A. Bychowska, K. Brzozowski, J. Thöming, P. Stepnowski, Application of spectroscopic methods for structural analysis of chitin and chitosan, Marine Drugs 8 (2010) 1567–1636.
[8] M. Bengisu, E. Yilmaz, Oxidation and pyrolysis of chitosan as a route for carbon fiber derivation, Carbohydrate Polymer 250 (2002) 165–175.
[9] A. Higazy, M. Hashema, A. Elshafei, N. Shakerc, M.A. Hady, Development of antimicrobial jute packaging using chitosan and chitosan–metal complex, Carbohydrate Polymer 79 (2010) 867–874.
[10] W.J. Tang, C.X. Wang, D.H. Chen, Kinetic studies on the pyrolysis of chitin and chitosan, Polymer Degradation and Stability 87 (2005) 389–394.
[11] C.Y. Ou, C.H. Zhang, S.D. Li, L. Yang, J.J. Dong, X.L. Mo, M.T. Zeng, Thermal degradation kinetics of chitosan–cobalt complex as studied by thermogravimetric analysis, Carbohydrate Polymer 82 (2010) 1284–1289.
[12] R.L. Patale, V.B. Patravale, O. N-carboxymethyl, chitosan–zinc complex: a novel chitosan complex with enhanced antimicrobial activity, Carbohydrate Polymer 85 (2011) 105–110.
[13] H.Y. Liu, X.Q. Hou, X.Q. Wang, Y.L. Wang, D. Xu, C. Wang, W. Du, M.K. Lü, D.R. Yuan, Fabrication of high-strength continuous zirconia fibers and their formation mechanism study, Journal of the American Ceramic Society 87 (12) (2004) 2237–2241.